



Efficient Spherical Harmonic Transforms aimed at pseudo-spectral numerical simulations

Nathanaël Schaeffer

► To cite this version:

Nathanaël Schaeffer. Efficient Spherical Harmonic Transforms aimed at pseudo-spectral numerical simulations. 2012. insu-00675145v2

HAL Id: insu-00675145

<https://insu.hal.science/insu-00675145v2>

Preprint submitted on 8 Dec 2012 (v2), last revised 4 Nov 2014 (v4)

HAL is a multi-disciplinary open access archive for the deposit and dissemination of scientific research documents, whether they are published or not. The documents may come from teaching and research institutions in France or abroad, or from public or private research centers.

L'archive ouverte pluridisciplinaire **HAL**, est destinée au dépôt et à la diffusion de documents scientifiques de niveau recherche, publiés ou non, émanant des établissements d'enseignement et de recherche français ou étrangers, des laboratoires publics ou privés.

Efficient Spherical Harmonic Transforms aimed at pseudo-spectral numerical simulations

Nathanaël Schaeffer

ISTerre, Université de Grenoble 1, CNRS, F-38041 Grenoble, France

December 8, 2012

Abstract

In this paper, we report on very efficient algorithms for the spherical harmonic transform (SHT). Explicitly vectorized variations of the Gauss-Legendre algorithm are discussed and implemented in the **SHTns** library which includes scalar and vector transforms. This library is especially suitable for direct numerical simulations of non-linear partial differential equations in spherical geometry, like the Navier-Stokes equation. The performance of our algorithms is compared to third party SHT implementations, including fast algorithms. Even though the complexity of the algorithms implemented in **SHTns** are in $\mathcal{O}(N^3)$ (where N is the maximum harmonic degree of the transform), they perform much better than the available implementations of asymptotically fast algorithms, even for a truncation as high as $N = 1023$. In our performance tests, the best performance for SHT is delivered by **SHTns**, which is available at <https://bitbucket.org/nschaeff/shtns> as open source software.

1 Introduction

Spherical harmonics are the eigenfunctions of the Laplace operator on the 2-sphere. They form a basis and are useful and convenient to describe data on a sphere in a consistent way in spectral space. Spherical Harmonic Transforms (SHT) are the spherical counterpart of the Fourier transform, casting spatial data to the spectral domain and vice versa. They are commonly used in various pseudo-spectral direct numerical simulations in spherical geometry, for simulating the Sun or the liquid core of the Earth among others Glatzmaier (1984); Sakuraba (1999); Christensen et al. (2001); Brun and Rempel (2009); Wicht and Tilgner (2010).

All numerical simulations that take advantage of spherical harmonics use the classical Gauss-Legendre algorithm (see section 2) with complexity $\mathcal{O}(N^3)$ for a truncation at spherical harmonic degree N . As a consequence of this high computational cost when N increases, high resolution spherical codes currently spend most of their time performing SHT. A few years ago, state of the art numerical simulations used $N = 255$ Sakuraba and Roberts (2009).

However, there exist several asymptotically fast algorithms (Driscoll and Healy, 1994; Potts et al., 1998; Mohlenkamp, 1999; Suda and Takami, 2002; Healy et al., 2003; Tygert, 2008), but the overhead for these fast algorithms is such that they do not claim to be effectively faster for $N < 512$. In addition, some of them lack stability (the error becomes too large even for moderate N) and flexibility (e.g. $N + 1$ must be a power of 2).

Among the asymptotically fast algorithm, only two have open-source implementations, and the only one which seems to perform reasonably well is **SpharmonicKit**, based on the algorithms described by Healy et al. (2003). Its main drawback is the need of a latitudinal grid of size $2(N + 1)$ while the Gauss-Legendre quadrature allows the use of only $N + 1$ collocation points. Thus, even if it were as fast as the Gauss-Legendre approach for the same truncation N , the overall numerical simulation would be slower because it would operate on twice as many points. These facts explain why the Gauss-Legendre algorithm is still the most efficient solution for numerical simulations.

A recent paper Dickson et al. (2011) reports that carefully tuned software could finally run 9 times faster on the same CPU than the initial non-optimized version, and insists on the importance of vectorization and careful optimization of the code. As the goal of this work is to speed-up numerical simulations, we have written a highly optimized and explicitly vectorized version of the Gauss-Legendre SHT algorithm. The next section recalls the basics of spherical harmonic transforms. We then describe the optimizations we use and we compare the performance of our transform to other SHT implementations. We conclude this paper by a short summary and perspectives for future developments.

2 Spherical Harmonic Transform (SHT)

2.1 Definitions and properties

The orthonormalized spherical harmonics of degree n and order $-n \leq m \leq n$ are functions defined on the sphere as:

$$Y_n^m(\theta, \phi) = P_n^m(\cos \theta) \exp(im\phi) \quad (1)$$

where θ is the colatitude, ϕ is the longitude and P_n^m are the associated Legendre polynomials normalized for spherical harmonics

$$P_n^m(x) = (-1)^m \sqrt{\frac{2n+1}{4\pi}} \sqrt{\frac{(n-|m|)!}{(n+|m|)!}} (1-x^2)^{|m|/2} \frac{d^{|m|}}{dx^{|m|}} P_n(x) \quad (2)$$

which involve derivatives of Legendre Polynomials $P_n(x)$ defined by the following recurrence:

$$\begin{aligned} P_0(x) &= 1 \\ P_1(x) &= x \\ nP_n(x) &= (2n-1)xP_{n-1}(x) - (n-1)P_{n-2}(x) \end{aligned}$$

The spherical harmonics $Y_n^m(\theta, \phi)$ form an orthonormal basis for functions defined on the sphere:

$$\int_0^{2\pi} \int_0^\pi Y_n^m(\theta, \phi) Y_l^k(\theta, \phi) \sin \theta d\theta d\phi = \delta_{nl} \delta_{mk} \quad (3)$$

with δ_{ij} the Kronecker symbol. By construction, they are eigenfunctions of the Laplace operator on the unit sphere:

$$\Delta Y_n^m = -n(n+1)Y_n^m \quad (4)$$

This property is very appealing for solving many physical problems in spherical geometry involving the Laplace operator.

2.2 Synthesis or inverse transform

The Spherical Harmonic synthesis is the evaluation of the sum

$$f(\theta, \phi) = \sum_{n=0}^N \sum_{m=-n}^n f_n^m Y_n^m(\theta, \phi) \quad (5)$$

up to degree $n = N$, given the complex coefficients f_n^m . If $f(\theta, \phi)$ is a real-valued function, $f_n^{-m} = (f_n^m)^*$, where z^* stands for the complex conjugate of z .

The sums can be exchanged, and using the expression of Y_n^m we can write

$$f(\theta, \phi) = \sum_{m=-N}^N \left(\sum_{n=|m|}^N f_n^m P_n^m(\cos \theta) \right) e^{im\phi} \quad (6)$$

From this last expression, it appears that the summation over m is a regular Fourier Transform. Hence the remaining task is to evaluate

$$f_m(\theta) = \sum_{n=|m|}^N f_n^m P_n^m(\cos \theta) \quad (7)$$

or its discrete version at given collocation points θ_j .

2.3 Analysis or forward transform

The analysis step of the SHT consists in computing the coefficients

$$f_n^m = \int_0^{2\pi} \int_0^\pi f(\theta, \phi) Y_n^m(\theta, \phi) \sin \theta d\theta d\phi \quad (8)$$

The integral over ϕ is obtained using the Fourier Transform:

$$f_m(\theta) = \int_0^{2\pi} f(\theta, \phi) e^{im\phi} d\phi \quad (9)$$

so the remaining Legendre transform reads

$$f_n^m = \int_0^\pi f_m(\theta) P_n^m(\cos \theta) \sin \theta d\theta \quad (10)$$

The discrete problem reduces to the appropriate quadrature rule to evaluate the integral (10) knowing only the values $f_m(\theta_j)$. In particular, the use of the Gauss-Legendre quadrature replaces the integral of expression 10 by the sum

$$f_n^m = \sum_{j=1}^{N_\theta} f_m(\theta_j) P_n^m(\cos \theta_j) w_j \quad (11)$$

where θ_j and w_j are respectively the Gauss nodes and weights Temme (2011). Note that the sum equals the integral if $f_m(\theta) P_n^m(\cos \theta)$ is a polynomial in $\cos \theta$ of order $2N_\theta - 1$ or less. If $f_m(\theta)$ is given by expression 7, then $f_m(\theta) P_n^m(\cos \theta)$ is always a polynomial in $\cos \theta$, of degree at most $2N$. Hence the Gauss-Legendre quadrature is exact for $N_\theta \geq N + 1$.

A discrete spherical harmonic transform using Gauss nodes as latitudinal grid points and a Gauss-Legendre quadrature for the analysis step is referred to as a Gauss-Legendre algorithm.

3 Optimization of the Gauss-Legendre algorithm

3.1 Standard optimizations

Let us first recall some standard optimizations found in almost every serious implementation of the Gauss-Legendre algorithm. All the following optimizations are used in the **SHTns** library.

Use the Fast-Fourier Transform The expressions of section 2 show that part of the SHT is in fact a Fourier transform. The fast Fourier transform (FFT) should be used for this part, as it improves accuracy and speed. **SHTns** uses the **FFTW** library Frigo and Johnson (2005), a portable, flexible and blazingly fast FFT implementation.

Take advantage of Hermitian symmetry for real data When dealing with real-valued data, the spectral coefficients verify $f_n^{-m} = (f_n^m)^*$, so we only need to store them for $m \geq 0$. This also allows the use of faster real-valued FFTs.

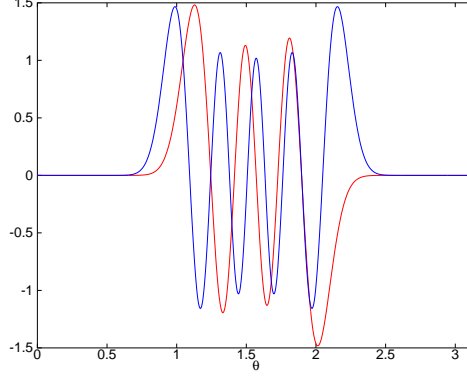


Figure 1: Two associated Legendre polynomials of degree $n = 40$ and order $m = 33$ (blue) and $m = 36$ (red), showing the localization near the equator.

Take advantage of mirror symmetry Due to the defined symmetry of spherical harmonics with respect to a reflection about the equator

$$P_n^m(\cos(\pi - \theta)) = (-1)^{n+m} P_n^m(\cos \theta)$$

one can reduce by a factor 2 the operation count of both forward and inverse transforms.

Precompute values of P_n^m The coefficients $P_n^m(\cos \theta_j)$ appear in both synthesis and analysis expressions (7 and 10), and can be precomputed and stored for all (n, m, j) . When performing multiple transforms, it avoids computing the Legendre polynomial recursion at every transform and saves some computing power, at the expense of memory bandwidth. This may or may not be efficient, as we will discuss later.

Polar optimization High order spherical harmonics have their magnitude decrease exponentially when approaching the poles as shown in figure 1. Hence, the integral of expression 10 can be reduced to

$$f_n^m = \int_{\theta_0^{mn}}^{\pi - \theta_0^{mn}} f_m(\theta) P_n^m(\cos \theta) \sin \theta d\theta \quad (12)$$

where $\theta_0^{mn} \geq 0$ is a threshold below which P_n^m is considered to be zero. Similarly, the synthesis of $f_m(\theta)$ (eq. 7) is only needed for $\theta_0^{mn} \leq \theta \leq \pi - \theta_0^{mn}$. **SHTns** uses a threshold θ_0^{mn} that does not depend on n , which leads to around 5% to 20% speed increase, depending on the desired accuracy and the truncation N .

3.2 On-the-fly algorithms and vectorization

It can be shown that $P_n^m(x)$ can be computed recursively by

$$P_m^m(x) = a_m^m (1 - x^2)^{|m|/2} \quad (13)$$

$$P_{m+1}^m(x) = a_{m+1}^m x P_m^m(x) \quad (14)$$

$$P_n^m(x) = a_n^m x P_{n-1}^m(x) + b_n^m P_{n-2}^m(x) \quad (15)$$

with

$$a_m^m = \sqrt{\frac{1}{4\pi} \prod_{k=1}^{|m|} \frac{2k+1}{2k}} \quad a_n^m = \sqrt{\frac{4n^2 - 1}{n^2 - m^2}} \quad b_n^m = -\sqrt{\frac{2n+1}{2n-3} \frac{(n-1)^2 - m^2}{n^2 - m^2}} \quad (16)$$

The coefficients a_n^m and b_n^m do not depend on x , and can be easily precomputed and stored into an array of $N(N+1)$ values. This has to be compared to the order N^3 values of $P_n^m(x_j)$, which are usually precomputed and stored in the spherical harmonic transforms implemented in numerical simulations. The amount of memory required to store all $P_n^m(x_j)$ in double-precision is at least $2(N+1)^3$ bytes, which gives 2Gb for $N = 1023$. When N becomes very large, it is no longer possible to store $P_n^m(x_j)$ in memory (for $N \gtrsim 1023$ nowadays) and on-the-fly algorithms (which recompute $P_n^m(x_j)$ from the recurrence relation when needed) are then the only possibility.

We would like to stress that even far from that storage limit, on-the-fly algorithm can be significantly faster thanks to vector capabilities of modern processors. Most desktop and laptop computers, as well as many high performance computing clusters, have support for Single-Instruction-Multiple-Data (SIMD) operations in double precision. The SSE2 instruction set is available since year 2000 and currently supported by almost every PC, allowing to perform the same double precision arithmetic operations on a vector of 2 double precision numbers, effectively doubling the computing power. The recently introduced AVX instruction set increases the vector size to 4 double precision numbers. This means that $P_n^m(x)$ can be computed from the recursion relation 15 (which requires 3 multiplications and 1 addition) for 2 or 4 values of x simultaneously, which may be faster than loading pre-computed values from memory. Hence, as already pointed out by Dickson et al. (2011), it is therefore very important to use the vector capabilities of modern processors to address their full computing power. Furthermore, when running multiple transforms on the different cores of a computer, the performance of on-the-fly transforms (which use less memory bandwidth) scales much better than algorithms with precomputed matrices, because the memory bandwidth is shared between cores. Superscalar architectures that do not have double-precision SIMD instructions but have many computation unit per core (like the POWER7 or SPARC64) could also benefit from on-the-fly transforms by saturating the many computation units with independent computations (at different x).

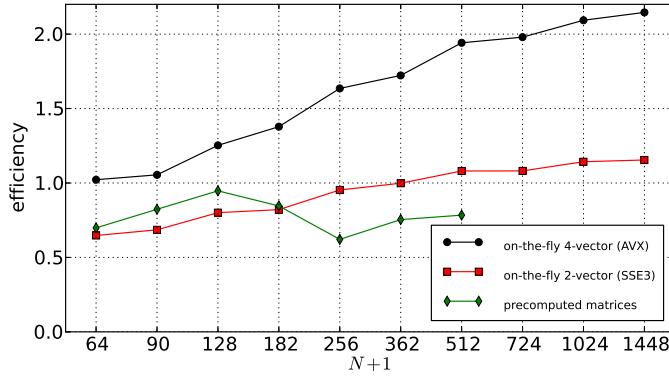


Figure 2: Efficiency $(N+1)^3/(2tf)$ of various algorithms, where t is the execution time and f the frequency of the Xeon E5-2680 CPU (2.7GHz). On-the-fly algorithms with two different vector sizes are compared with the algorithm using precomputed matrices. Note the influence of hardware vector size for on-the-fly algorithms (AVX vectors pack 4 double precision floating point numbers where SSE3 vectors pack only 2). The efficiency of the algorithm based on precomputed matrices drops above $N = 127$ probably due to cache size limitations.

Figure 2 shows the benefit of explicit vectorization of on-the-fly algorithms on an intel Xeon E5-2680 (*Sandy Bridge* architecture with AVX instruction set running at 2.7GHz) and compares on-the-fly algorithms with algorithms based on precomputed matrices. With the 4-vectors of AVX, the fastest algorithm is always on-the-fly, while for 2-vectors, the fastest algorithm uses precomputed matrices for $N \lesssim 200$.

Runtime tuning We have now two different available algorithms: one uses precomputed values for $P_n^m(x)$ and the other one computes them on-the-fly at each transform. The SHTns library

compares the time taken by those algorithms (and variants) at startup and chooses the fastest, similarly to what the FFTW library Frigo and Johnson (2005) does. In the forthcoming years, AVX will become widely available, and the benefits of on-the-fly vectorized transforms will become even more important.

3.3 Multi-threaded transform

Modern computers have several computing cores. We used OpenMP to implement a multi-threaded algorithm for the Legendre transform including the above optimization and the *on-the-fly* approach. The lower memory bandwidth requirements for the *on-the-fly* approach is an asset for a multi-threaded transform because if each thread would read a different portion of a large matrix, it can saturate the memory bus very quickly. The multi-threaded Fourier transform is left to the FFTW library.

We need to decide how to share the work between different threads. Because we compute the P_n^m on the fly using the recurrence relation 15, we are left with each thread computing different θ , or different m . As the analysis step involve a sum over θ , we choose the latter option.

From equation 7, we see that the number of terms involved in the sum depends on m , so that the computing cost will also depend on m . In order to achieve the best workload balance between a team of p threads, the thread number i ($0 \leq i < p$) handles $m = i + kp < n$, with integer k from 0 to n/p .

For different thread number b , we have measured the time $T_s(p)$ and $T_a(p)$ needed for a scalar spherical harmonic synthesis and analysis respectively (including the FFT).

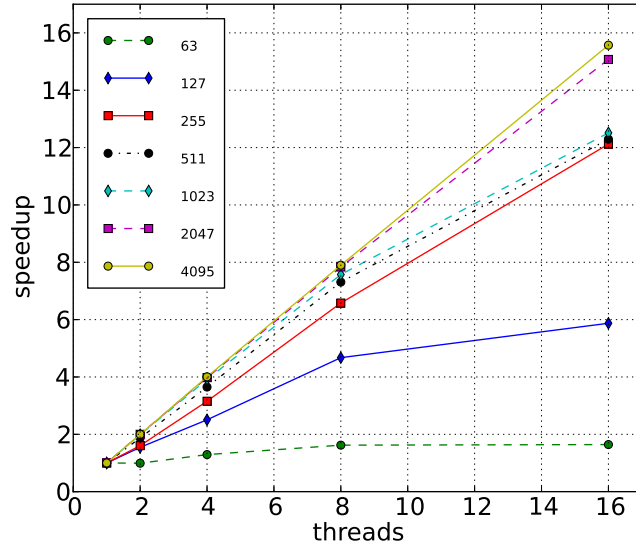


Figure 3: Speedup obtained with multiple threads using OpenMP on a 16 core intel Xeon E5-2680 (*Sandy Bridge* architecture with AVX instruction set running at 2.7 GHz).

Figure 3 shows the speedup $T(1)/T(p)$, where $T(p)$ is the largest of $T_s(p)$ and $T_a(p)$ and $T(1)$ is the time of the fastest single threaded transform. It shows that there is no point in doing a parallel transform with ℓ_{max} below 128. The speedup is good for $\ell_{max} = 255$ or above, and excellent up to 8 threads for $\ell_{max} \geq 511$ or up to 16 threads for very large transform ($\ell_{max} \geq 2047$).

3.4 Performance comparisons

Table 1 reports the timing measurements of two SHT libraries, compared to the optimized Gauss-Legendre implementation found in the SHTns library (this work). We compare with the Gauss-

N	63	127	255	511	1023	2047	4095
libpsht (1 thread)	1.05 ms	4.7 ms	27 ms	162 ms	850 ms	4.4 s	30.5 s
DH (fast)	1.1 ms	5.5 ms	21 ms	110 ms	600 ms	NA	NA
SHTns (1 thread)	0.09 ms	0.60 ms	4.2 ms	28 ms	216 ms	1.6 s	11.8 s

Table 1: Comparison of execution time for different SHT implementations. The numbers correspond to the average execution time for forward and backward scalar transform (including the FFT) on an Intel Xeon X5650 (2.67GHz) with 12 cores. The programs were compiled with `gcc 4.4.5` and `-O3 -march=native -ffast-math` compilation options.

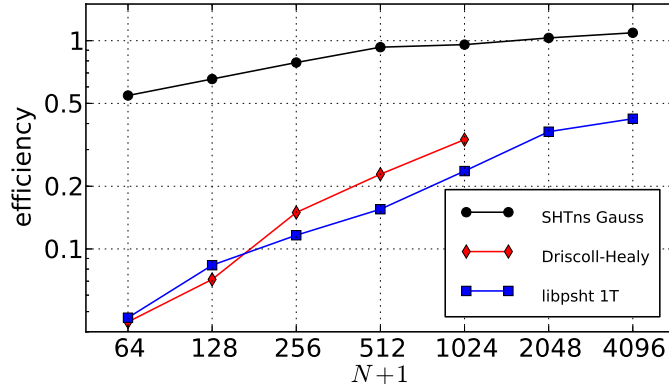


Figure 4: Efficiency $(N+1)^3/(2Tf)$ of the implementations from table 1, where T is the execution time and f the frequency of the Xeon X5650 CPU (2.67GHz) with 12 cores.

Legendre implementation of **libpsht** (Reinecke, 2011), a parallel spherical harmonic transform library targeting very large N , and with **SpharmonicKit** 2.7 (DH) which implements one of the Driscoll-Healy fast algorithms Healy et al. (2003). All the timings are for a complete SHT, which includes the Fast Fourier Transform. Note that the Gauss-Legendre algorithm is by far (a factor of order 2) the fastest algorithm of the **libpsht** library. Note also that **SpharmonicKit** is limited to $N+1$ being a power of two, requires $2(N+1)$ latitudinal colocation points, and crashed for $N = 2047$. The software library implementing the fast Legendre transform described in Mohlenkamp (1999), **libftsh**, has also been tested, and found to be of comparable performance to that of **SpharmonicKit**, although the comparison is not straightforward because **libftsh** did not include the Fourier Transform. Again, that fast library could not operate at $N = 2047$ because of memory limitations. Note finally that these measurements were performed on a machine that did not support the new AVX instruction set.

In order to ease the comparison, we define the efficiency of the SHT by $(N+1)^3/(2Tf)$, where T is the execution time (reported in table 1) and f the frequency of the CPU. Note that $(N+1)^3/2$ reflects the number of computation elements of a Gauss-Legendre algorithm (the number of modes $(N+1)(N+2)/2$ times the number of latitudinal points $N+1$). An efficiency that does not depend on N corresponds to an algorithm with an execution time proportional to N^3 .

The efficiency of the tested algorithms are displayed in figure 4. Not surprisingly, the Driscoll-Healy implementation has the largest slope, which means that its efficiency grows fastest with N , as expected for a fast algorithm. It also performs slightly better than **libpsht** for $N \geq 511$. However, even for $N = 1023$ (the largest size that it can compute), it is still 2.8 times slower than the Gauss-Legendre algorithm implemented in **SHTns**. It is remarkable that **SHTns** achieves an efficiency very close to 1, meaning that almost one element per clock cycle is computed for $N = 511$ and $N = 1023$. Overall, **SHTns** is between two and ten times faster than the best alternative.

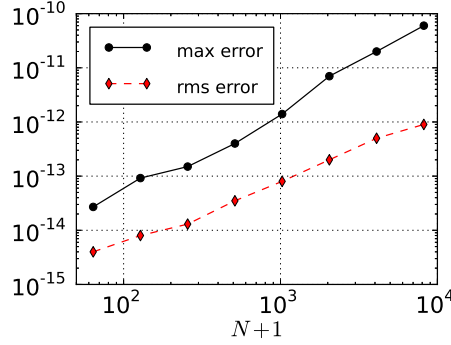


Figure 5: Accuracy of the on-the-fly Gauss-Legendre algorithm with the default polar optimization.

3.5 Accuracy

One cannot write about an SHT implementation without addressing its accuracy. Here, the Gauss-Legendre quadrature ensures very good accuracy, at least on par with other high quality implementations. To quantify the error we start with random spherical harmonic coefficients Q_l^m with each real part and imaginary part between -1 and $+1$. After a backward and forward transform (with orthonormal spherical harmonics), we compare the resulting coefficients R_l^m with the originals Q_l^m . We use two different error measurements: the maximum error is defined as

$$\epsilon_{max} = \max_{l,m} |R_l^m - Q_l^m|$$

while the root mean square (rms) error is defined as

$$\epsilon_{rms} = \sqrt{\frac{2}{(N+1)(N+2)} \sum_{l,m} |R_l^m - Q_l^m|^2}$$

The error measurements for our on-the-fly Gauss-Legendre implementation with the default polar optimization and for various truncation degree N are shown in figure 5. The errors steadily increase with N and are comparable to other implementations. For $N < 2048$ we have $\epsilon_{max} < 10^{-11}$, which is negligible compared to other sources of errors in most numerical simulations.

4 Conclusion and perspectives

Despite the many fast spherical harmonic transform algorithms published, the few with a publicly available implementation are far from the performance of a carefully written Gauss-Legendre algorithm, as implemented in the **SHTns** library, even for quite large truncation ($N = 1023$). Explicitly vectorized on-the-fly algorithm seem to be able to unleash the computing power of nowadays and future computers, without suffering too much of memory bandwidth limitations, which is an asset for multi-threaded transform. Finally, by choosing at runtime the fastest available SHT algorithm, the **SHTns** library will most certainly deliver the fastest spherical transform to your platform. The versatile truncation, the various normalization conventions supported, as well as the scalar and vector transform routines available for C/C++, Fortran or Python, should suit most of the current and future needs in high performance computing involving partial differential equations in spherical geometry.

Acknowledgements

The author thanks Alexandre Fournier and Daniel Lemire for their comments that helped to improve the paper. Some computations have been carried out at the Service Commun de Cal-

cul Intensif de l'Observatoire de Grenoble (SCCI) and other were run on the PRACE Research Infrastructure *Curie* at the TGCC (grant PA1039).

References

- Brun, A., Rempel, M., Apr. 2009. Large scale flows in the solar convection zone. *Space Science Reviews* 144 (1), 151–173.
URL <http://dx.doi.org/10.1007/s11214-008-9454-9>
- Christensen, U. R., Aubert, J., Cardin, P., Dormy, E., Gibbons, S., Glatzmaier, G. A., Grote, E., Honkura, Y., Jones, C., Kono, M., Matsushima, M., Sakuraba, A., Takahashi, F., Tilgner, A., Wicht, J., Zhang, K., Dec. 2001. A numerical dynamo benchmark. *Physics of The Earth and Planetary Interiors* 128 (1-4), 25–34.
URL [http://dx.doi.org/10.1016/S0031-9201\(01\)00275-8](http://dx.doi.org/10.1016/S0031-9201(01)00275-8)
- Dickson, N. G., Karimi, K., Hamze, F., Jun. 2011. Importance of explicit vectorization for CPU and GPU software performance. *Journal of Computational Physics* 230 (13), 5383–5398.
URL <http://dx.doi.org/10.1016/j.jcp.2011.03.041>
- Driscoll, J., Healy, D. M., June 1994. Computing fourier transforms and convolutions on the 2-sphere. *Advances in Applied Mathematics* 15 (2), 202–250.
URL <http://dx.doi.org/10.1006/aama.1994.1008>
- Frigo, M., Johnson, S. G., Feb. 2005. The design and implementation of FFTW3. *Proceedings of the IEEE* 93 (2), 216–231.
URL <http://www.fftw.org/fftw-paper-ieee.pdf>
- Glatzmaier, G. A., Sep. 1984. Numerical simulations of stellar convective dynamos. i. the model and method. *Journal of Computational Physics* 55 (3), 461–484.
URL [http://dx.doi.org/10.1016/0021-9991\(84\)90033-0](http://dx.doi.org/10.1016/0021-9991(84)90033-0)
- Healy, D. M., Rockmore, D. N., Kostelec, P. J., Moore, S., July 2003. Ffts for the 2-sphere-improvements and variations. *Journal of Fourier Analysis and Applications* 9 (4), 341–385.
URL <http://dx.doi.org/10.1007/s00041-003-0018-9>
- Mohlenkamp, M. J., 1999. A fast transform for spherical harmonics. *The Journal of Fourier Analysis and Applications* 5 (2/3).
URL <http://www.springerlink.com/content/n01v8q03m5584253/>
- Potts, D., Steidl, G., Tasche, M., Oct. 1998. Fast algorithms for discrete polynomial transforms. *Mathematics of Computation* 67, 1577–1590.
URL <http://adsabs.harvard.edu/abs/1998MaCom...67.1577P>
- Reinecke, M., Feb. 2011. Libpsht – algorithms for efficient spherical harmonic transforms. *Astronomy & Astrophysics* 526, A108+.
URL <http://arxiv.org/abs/1010.2084>
- Sakuraba, A., Feb. 1999. Effect of the inner core on the numerical solution of the magnetohydrodynamic dynamo. *Physics of The Earth and Planetary Interiors* 111 (1-2), 105–121.
URL [http://dx.doi.org/10.1016/S0031-9201\(98\)00150-2](http://dx.doi.org/10.1016/S0031-9201(98)00150-2)
- Sakuraba, A., Roberts, P. H., Oct. 2009. Generation of a strong magnetic field using uniform heat flux at the surface of the core. *Nature Geoscience* 2 (11), 802–805.
URL <http://dx.doi.org/10.1038/ngeo643>
- Suda, R., Takami, M., 2002. A fast spherical harmonics transform algorithm. *Mathematics of Computation* 71 (238), 703–715.
URL <http://dx.doi.org/10.1090/S0025-5718-01-01386-2>

- Temme, N. M., Aug. 2011. Gauss quadrature. In: Digital Library of Mathematical Functions (DLMF). National Institute of Standards and Technology (NIST), Ch. 3.5(v).
URL <http://dlmf.nist.gov/3.5.v>
- Tygart, M., Jan. 2008. Fast algorithms for spherical harmonic expansions, II. Journal of Computational Physics 227 (8), 4260–4279.
URL <http://dx.doi.org/10.1016/j.jcp.2007.12.019>
- Wicht, J., Tilgner, A., May 2010. Theory and modeling of planetary dynamos. Space Science Reviews 152 (1), 501–542.
URL <http://dx.doi.org/10.1007/s11214-010-9638-y>